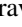






Models of cosmological black holes

Pravin K. Dahal ^{*}, Swayamsiddha Maharana [†], Fil Simovic [‡], Ioannis Soranidis [§], and Daniel R. Terno [¶]
School of Mathematical and Physical Sciences, Macquarie University, NSW 2109, Australia

We study various aspects of modeling astrophysical black holes using the recently introduced semiclassical formalism of physical black holes (PBHs). This approach is based on the minimal requirements of observability and regularity of the horizons. We demonstrate that PBHs do not directly couple to the cosmological background in the current epoch, and their equation of state renders them unsuitable for describing dark energy. Utilizing their properties for analysis of more exotic models, we present a consistent semiclassical scenario for a black-to-white hole bounce and identify obstacles to the transformation from a black hole horizon to a wormhole mouth.

Introduction.— More than a hundred astrophysical black holes (ABHs) — dark, massive, ultra-compact objects — have been identified [1–4]. All observations are well-described by the classical Kerr solution to Einstein-Hilbert gravity [2, 4, 5]. This consistency is not yet a demonstration of key black hole features, such as light trapping. Moreover, a literal identification of ABHs with classical black hole solutions requires addressing singularities and unresolved semiclassical issues. This tension motivates development of the alternative ABH models, many of which are observationally viable [5, 6].

A rough classification scheme differentiates ABH models with horizons from their horizonless counterparts. The event horizon, a null surface that causally disconnects the black hole’s interior from the outside world [7, 8], is the defining feature of a mathematical black hole (MBH) [9]. Physical black holes (PBHs) [9] are trapped spacetime regions, potentially transient and not always overlapping with MBHs [10]. In contrast, various models describe ABHs without introducing horizons [5]. Distinguishing among ABH models remains one of the central problems in black hole physics [6].

In fact, we should distinguish three possibilities [10, 11]. From a distant observer’s point of view, gravitational collapse beyond neutron star density can result in either: (i) Ongoing collapse, with a horizon as an asymptotic ($t \rightarrow \infty$) concept. Under broad conditions (the energy conditions discussed below), MBHs are gravitational collapse’s asymptotic states [7, 8]; (ii) Formation of a transient or stable object, where a suitably-defined deviation from r_g reaches a minimum $\varepsilon > 0$ [5]. Black hole mimickers fall into this category; (iii) Formation of an apparent horizon in finite t_f . PBHs, subject to this requirement, fall into this category [10, 12]. The same alternatives arise in mergers.

Here, we investigate the consequences of accepting option (iii). After describing PBHs, we analyse their direct coupling with cosmological dynamics, identify a viable black-to-white hole transition scenarios, and present the obstacles in forming traversable wormholes. It is noteworthy that, like most conceptual and observational black hole discussions, our analysis is framed within the semiclassical framework. Thus, our conclusions serve both as a list of PBH features, and as indicators of potential breakdown of semiclassical gravity on a macroscopic scale.

Semiclassical black and white holes. — Our formalism is

based on two premises. First, the spacetime geometry can be described using a metric $g_{\mu\nu}$ with classical concepts of horizons, trajectories, and the equations that describe them remaining valid. Second, we assume the metric $g_{\mu\nu}$ is a solution to the semiclassical Einstein equations [13–15]

$$G_{\mu\nu} = 8\pi \langle \hat{T}_{\mu\nu} \rangle_\omega, \quad (1)$$

where the left hand side is the Einstein tensor $G_{\mu\nu} = R_{\mu\nu} - \frac{1}{2}Rg_{\mu\nu}$, and the right hand side is the effective energy-momentum tensor (EMT), $\langle \hat{T}_{\mu\nu} \rangle_\omega \equiv T_{\mu\nu}$. It includes the renormalized expectation value of all matter fields, higher-order terms arising from its regularisation, and possible contributions arising from modifications to the Einstein-Hilbert gravity or a cosmological constant Λ . In the subsequent analysis we do not use any specific property of the state ω and do not separate the matter EMT into the collapsing matter and (perturbatively-obtained) quantum excitations.

In discussing PBH properties [10], we apply the weakest form of the cosmic censorship and require absence of scalar curvature singularities at the apparent horizon [7]. Unlike the teleological event horizon, the apparent horizon is in principle observable [16]. We express this observability by requiring a finite formation time according to the clocks of distant observers [10, 17].

Most of our discussion is restricted to spherical symmetry, where the two above assumptions lead to the exhaustive classification of allowed metrics and to clarification of some key features of the black hole formation and the near-horizon geometry. We will also use Kerr–Vaidya black holes as the simplest example of axially-symmetric dynamical models [18, 19].

A general spherically symmetric metric in Schwarzschild coordinates (r is the areal radius) is given by

$$ds^2 = -e^{2h(t,r)} f(t,r) dt^2 + f(t,r)^{-1} dr^2 + r^2 d\Omega_2, \quad (2)$$

while using the advanced null coordinate v results in the form

$$ds^2 = -e^{2h_+(v,r)} f_+(v,r) dv^2 + 2e^{h_+(v,r)} dv dr + r^2 d\Omega_2. \quad (3)$$

The function f is coordinate-independent, i.e. $f(t,r) \equiv f_+(v(t,r),r)$ and in what follows we omit the subscript. It

is conveniently represented via the Misner–Sharp–Hernandez (MSH) mass $M_M \equiv C_M/2$ [20] as

$$f = 1 - \frac{C_M(t, r)}{r} = 1 - \frac{C_+^M(v, r)}{r} = \partial_\mu r \partial^\mu r, \quad (4)$$

The functions h and h_+ play the role of integrating factors in the coordinate transformation

$$dt = e^{-h}(e^{h_+} dv - f^{-1} dr). \quad (5)$$

For example, the Schwarzschild metric corresponds to $h \equiv 0$, $C_M \equiv r_g = \text{const}$, and $v = t + r_*$, where r_* is the tortoise coordinate [7, 8], while the de Sitter metric in the static patch is given by $h \equiv 0$, $C_M = H^2 r^3$, where H is the constant Hubble parameter [20, 21].

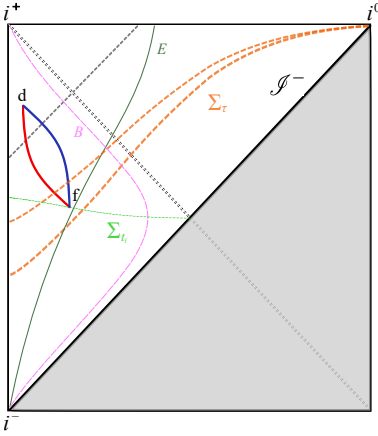


FIG. 1. Schematic Carter–Penrose diagram depicting the formation and evaporation of a regular black hole in a de Sitter spacetime [12]. Past and future timelike infinity are labelled by i^- and i^+ , respectively. Spacelike infinity is labelled by i^0 . Dashed grey lines correspond to outgoing radial null geodesics. The trajectory of a distant observer is indicated in pink and labelled B . The points f and d represent the two-spheres of formation and disappearance of the trapped region. The equal (Schwarzschild) time hypersurface Σ_{t_f} is shown as a dashed light green line. The outer (blue) and inner (dark red) components of the black hole apparent horizon (timelike membranes) are indicated according to the invariant definition [10, 20]. The invariantly-defined components of the apparent horizon correspond the largest and smallest root of $f = 0$ whether t , v or u is used as the evolution parameter. The solid black line connecting i^- and i^0 represents the cosmological event horizon for an observer at $r = 0$. Static coordinates cover only the left quadrant, with the dotted diagonal line representing the particle horizon. Components of the black hole apparent horizon correspond to the largest and smallest roots of $f = 0$ (not including the cosmological horizon). The orange dashed lines Σ_τ indicate hypersurfaces of constant cosmological time τ . The trajectory of an asymptotically comoving observer ($\chi = \text{const}$) is marked by the dark green line and labelled by the initial E .

In a cosmological setting (such as depicted on Fig. 1), we assume that a separation of scales exists between geometric features associated with the black hole and those of the large-scale universe [12]. In this case, the apparent horizons of the PBH is given by the real roots of $f(t, r) = 0$ in the near-

region [10]. The largest such root is the Schwarzschild radius r_g that represents the location of the outer black hole horizon. Invariance of the MSH mass implies

$$r_g(t) = r_+(v(t, r_g(t))), \quad (6)$$

where r_+ is the equivalent root of $f(v, r)$. Unlike the globally defined event horizon, the apparent horizon is foliation-dependent. However, it is invariantly defined in all foliations that respect spherical symmetry [22] which will be used in the following.

In preparation for the study of a PBH as an inhomogeneity on the cosmological background, described by Λ -Cold Dark Matter [23], we set

$$T_{\mu\nu} = T_{\mu\nu}^{\text{mat}} - \Lambda g_{\mu\nu}/8\pi, \quad (7)$$

separating the EMT into the matter and the cosmological constant parts, respectively. Both the Einstein equations and the regularity requirements are most conveniently written if we introduce the effective EMT components

$$\tau_t := e^{-2h} T_{tt} = \tau_t^{\text{mat}} + \Lambda f/8\pi, \quad (8)$$

$$\tau^r := T^{rr} = \tau_{\text{mat}}^r - \Lambda f/8\pi, \quad (9)$$

$$\tau_t^r := e^{-h} T_t^r = \tau_t^{\text{mat}r}. \quad (10)$$

The Einstein equations for the components G_{tt} , G_t^r , and G^{rr} are then, respectively

$$\partial_r C_M = 8\pi r^2 \tau_t^{\text{mat}}/f + \Lambda r^2, \quad (11)$$

$$\partial_t C_M = 8\pi r^2 e^h \tau_t^{\text{mat}}, \quad (12)$$

$$\partial_r h = 4\pi r (\tau_t^{\text{mat}} + \tau_{\text{mat}}^r)/f^2. \quad (13)$$

Hence the most general metric that describes the cosmological embedding of a spherical inhomogeneity into spatially flat de Sitter spacetime is given by Eq. (2) with

$$C_M = C(t, r) + H^2 r^3, \quad (14)$$

where C (formally) satisfies the Einstein equations without the cosmological constant and $H = \sqrt{\Lambda/3}$.

To enforce the regularity condition it is sufficient to ensure that only the curvature scalars R and $R_{\mu\nu}R^{\mu\nu}$ are finite [10]. Moreover, the cosmological constant drops out of the key equations, and the analysis is performed along the usual lines of the self-consistent approach [10] (see Supplementary Material). As a result, C and C_M have the same structure [12] as $r \rightarrow r_g$. There are two admissible classes of the near-horizon solutions that are distinguished by the scaling of the effective EMT components as f^k , $k = 0, 1$ when $r \rightarrow r_g$.

The three components scale for the generic ($k = 0$) solution as

$$\tau_t, \tau^r \rightarrow -\Upsilon^2, \quad \tau_t^r \rightarrow \pm \Upsilon^2, \quad (15)$$

for some $\Upsilon(t)$. The two metric functions are

$$C = r_g - 4\sqrt{\pi}r_g^{3/2}\Upsilon\sqrt{x} + \mathcal{O}(x), \quad h = -\frac{1}{2}\ln\frac{x}{\xi} + \mathcal{O}(\sqrt{x}), \quad (16)$$

where $x := r - r_g(t)$, and the function $\xi(t)$ is determined by the choice of the time variable.

Consistency of the Einstein equations requires that

$$\frac{dr_g}{dt} \equiv r'_g = \pm 4\Upsilon\sqrt{\pi r_g \xi}, \quad (17)$$

where the plus (minus) sign corresponds to expansion (contraction) of the Schwarzschild radius. The case of $r'_g < 0$ is most conveniently described using the advanced null coordinate v . Evaluation of the expansions of null geodesic congruences [7, 20] identifies the domain $f < 0$ as a trapped region, and thus a PBH. The case of $r'_g > 0$ is most conveniently described using the retarded null coordinate u . In this case the domain $f < 0$ is the anti-trapped region, and we call the resulting entity a physical white hole (PWH) [10].

The function $\Upsilon^2(t) > 0$ determines the energy density at the apparent horizon, and the higher-order terms are matched with higher-order terms in the EMT expansion [10]. Both solutions violate the null energy condition (NEC) [7, 24], i.e. there are null vectors k^μ such that $T_{\mu\nu}k^\mu k^\nu < 0$. This is consistent with the result [7, 8] that the apparent horizon is not ‘visible’ to a distant observer unless the NEC is violated.

In both cases, the hypersurfaces $r = r_g$ are timelike. Therefore, both null (as indicated by Eq. (17)) and sufficiently fast massive test particles can enter a PBH in finite time t . The same applies to a PWH, although the analysis is somewhat more complex [19].

Regular black holes (RBHs) are non-singular PBHs. As such, they must have an inner horizon, which can be either timelike or null [25]. Analysis that is similar to the above shows that it is then a timelike hypersurface and the NEC is satisfied in its vicinity [26, 27]. The horizons do not joint smoothly, enabling the foliation-independent characterisation of the inner and outer segments [12, 27].

Two properties are crucial for the following. First, after formation of a spherically symmetric PBH, its outer apparent horizon can only contract, meaning the PBH mass decreases. Conversely, a PWH can only grow. In axially symmetric models like Kerr–Vaidya black holes, the situation is more complex. Expansion of the apparent horizon in (v, r) coordinates and contraction of the anti-trapping horizon in (u, r) coordinates are not obviously excluded. Nevertheless, Ref. [19] identifies two issues. During a black hole’s growth, signals from the apparent horizon cannot cross the hypersurface $r = M(v) + \sqrt{M^2(v) - a^2}$, which for expanding black holes is spacelike and screens the apparent horizon. Some white hole spacetimes with decreasing $M(u)$ are timelike geodesically incomplete.

Second, the equation of state near the apparent or anti-trapping horizon is $\rho = p$. For small angular momentum values, this applies to Kerr–Vaidya black holes. At the outer

horizon, both energy density and pressure are negative, while at the inner horizon, they are positive. Therefore, the PBH equation of state is more exotic than the de Sitter vacuum $\rho = -p > 0$ that is used as a core in a variety of models [5].

Cosmological coupling of black holes.— Within sub-percent precision the Universe is described at cosmological scales by spatially flat Friedmann–Lemaître–Robertson–Walker (FLRW) metric [23, 28]

$$ds^2 = -d\tau^2 + a^2(\tau)(d\chi^2 + \chi^2 d\Omega_2), \quad (18)$$

where χ is the comoving distance, τ the cosmic standard time, and $a(\tau)$ the scale factor. The Hubble parameter $H := \dot{a}/a$. In the present Λ -dominated epoch this geometry is well-approximated by the spatial flat de Sitter metric with $a(\tau) = H^{-1}\exp(H\tau)$.

Smaller scale inhomogeneities, including embedding of the black holes in this cosmological background [20, 21, 29] are active research subjects. In particular, the question whether black holes are affected by the large-scale dynamics of the cosmological background [30] was recently revisited. It was proposed in Ref. [31] that the black hole masses vary with the scale factor according to

$$M(a) = M(a_{\text{in}}) \left(\frac{a}{a_{\text{in}}} \right)^q, \quad (19)$$

where $a_{\text{in}} < a$ is the scale factor at which the object becomes cosmologically coupled, and a is its current value.

Ref. [32] then reported a value $q = 3.11_{-1.33}^{+1.19}$, and a strong confidence in excluding $q = 0$. This growth is immediately consistent with a cosmological vacuum equation of state $\rho = -p$ and thus black holes are a source of the dark energy. These conclusions, however, were criticised on both observational [33–36] and theoretical [30, 36–39] grounds.

The known explicit embedding models (Schwarzschild–Kottler–de Sitter, McVittie [20, 21] and Kerr–de Sitter [29] show no cosmological coupling [30, 39]. Analysis of general scenarios typically focuses on coupling of the cosmological background to local, spherically symmetric objects, since the black hole angular momentum effects are expected to be negligible on cosmological scales [30]. Despite ambiguity of black hole definitions (MBH and PBH are just two of them, see Ref. [40] for the discussion), in spherical symmetry a quasi-local MSH mass, that coincides with the Hawking–Hayward mass, is the preferred quantity [30, 36]. Moreover, it is directly tied to the notion of a PBH, as $M_{\text{M}} \equiv r_g/2$. Hence Eq. (19) implies

$$\frac{dr_g}{da} = \frac{\dot{r}_g}{\dot{a}} = q \frac{r_g}{a}, \quad (20)$$

where derivatives both of the Schwarzschild radius and the scale factor are taken with respect to the cosmological time.

As a result

$$\frac{dr_g}{da} = \frac{\dot{r}_g}{aH} \approx \frac{r'_g}{r_g} \frac{r_g}{H a}, \quad (21)$$

where we assumed that the distant observer is in the asymptotically de Sitter region but still far from the cosmological horizon, i.e. $r_g \ll r \ll H^{-1}$ and in this case $dt \approx d\tau$. Eq. (17) implies that dr_g/da is then negative. So long as the evaporation does not dramatically deviate from the Hawking–Page form [8] $r'_g \propto r_g^{-2}$, at the current epoch $1 \gg |q| \sim 0$. On the other hand, for the primordial black holes at the end of inflation and/or early radiation-dominated epochs [23, 41, 42] (that are treated as PBHs), the cosmological coupling can be strong.

Black-to-white hole bounce.— The idea that quantum effects can prevent black hole singularity from forming can be realised in several ways. For example, reformulating the one-loop corrections as effectively modifying the Lagrangian to fourth order, and collapse of a thin null shell results in transient, even if long-lived, trapped region [43]. Loop quantum gravity (LQG) corrections [44, 45], similarly to their effect in quantum cosmology, modify the collapse (for example, by introducing additional terms the classical Oppenheimer–Snyder collapse [45, 46] leading to the singularity avoidance and transient trapped region.

Over the past decade, there has been a resurgence in interest in white hole solutions, once considered less physically relevant predictions of general relativity [7, 8, 20]. Black-to-white hole transition scenarios [46–55] have elevated their status. Two versions are discussed [52, 53, 55]: “fireworks” [48] and “Planck stars” [49], both modeled as tunneling processes with differing characteristic times t_T . In the former, tunneling probability is of the order $\exp(-M^2/m_{\text{Pl}}^2)$, thus $t_T \sim M^2$, with $M = r_g/2$ as the pre-transition black hole mass and m_{Pl} the Planck mass. Since the Hawking–Page evaporation time scales as r_g^3 , black and white holes are macroscopic, and Hawking radiation effects are negligible. Recently, an LQG-inspired modification of the Oppenheimer–Snyder model was described [55], featuring a single asymptotic region with a complete, singularity-free Lorentzian metric that satisfies Einstein equations up to the tunneling region. In the latter scenario, $t_T \sim M^3$, with tunneling occurring after the black hole shrinks to about m_{Pl} . This potentially long-lived Planck-scale remnant is suggested as a dark matter component [51].

Regardless of scenario specifics, it is agreed that the transition occurs in a regime where semiclassical physics breaks down [46, 47]. However, significant parts of both black and white hole domains are described semiclassically. Depending on their specifics, bounce scenarios may involve space-like and timelike horizon segments, as well as a constant final white hole mass. Our approach limits these possibilities. Fig. (2) shows a modified semiclassical Penrose diagram of the black-to-white hole transition with a single asymptotic region based on this model. Within the validity domain of semiclassical gravity, objects before and after the bounce are

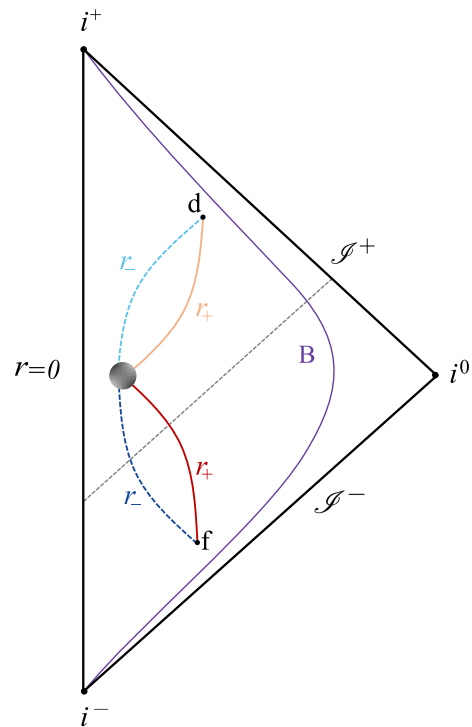


FIG. 2. A schematic Carter–Penrose diagram for the formation of a black hole, transition to a white hole, and subsequent disappearance. Semiclassical violation of the NEC implies timelike apparent trapping and anti-trapping horizons and a finite lifetime of the resulting white hole.

PBH and PWH, respectively. While agnostic about the actual bounce mechanism, the timelike nature of PBH’s inner and outer apparent horizons determines the pre-bounce structure. As only $r'_g > 0$ white hole solutions are allowed, growth termination requires closing the anti-trapped region, leading to a massive object. Its subsequent evolution is undefined in our model, but it is momentarily singularity-free and contains neither trapped nor anti-trapped regions.

Wormholes.— A traversable wormhole (TWH) is a hypothetical shortcut in spacetime that connects two distant regions of our Universe or two separate Universes [56, 57]. As the NEC violation [57, 63] and closed timelike curves are their unavoidable attributes, their primary use was in the realm of science fiction. However, in the last two decades they are considered as another class of ABH models [5, 58–61] their potential observational signatures are investigated [5, 59].

The original wormhole solutions were characterized using the embedding diagrams and explicit description of the two spatial sheets that are connected at the wormhole’s throat. Wormhole metrics are often written using the Schwarzschild coordinates on each sheet,

$$ds^2 = -e^\Phi dt^2 + \frac{dr^2}{1 - C/r} + r^2 d\Omega_2, \quad (22)$$

where Φ is a regular function and $r \geq b_0 > 0$, where b_0 is the (largest) root of $C(t, r) = r$ [57] that defines the worm-

hole throat. The invariant characterization of the throat that is valid for generic wormholes identifies it as an outer marginal trapped surface subject to additional conditions [63–65], allowing to use our formalism [66].

Consider a dynamical generalisation [62] of the Simpson–Visser metric [60] that is obtained by rewriting it in the retarded or advanced coordinates $w = u, v$ and allowing the mass parameter to depend it,

$$ds^2 = - \left(1 - \frac{2M(w)}{\sqrt{\eta^2 + a^2}} \right) dw^2 - 2\epsilon dw d\eta + (\eta^2 + a^2) d\Omega_2. \quad (23)$$

Here $a \geq 0$ is a parameter, $-\infty < \eta < +\infty$, and $\epsilon = \pm 1$ for $w = u, v$, respectively. As $r = \sqrt{\eta^2 + a^2} \geq a$, the MSH mass is $C_M = 2M + a^2(r - 2M)/r^2$.

This metric represents the Schwarzschild spacetime for $a = 0$, a regular black or white hole (also known as a black bounce) for $a < 2M$, and a traversable wormhole for $a > 2M$ [62]. In the former case, the Schwarzschild radius $r_e(w) = a \equiv b_0$ marks the wormhole throat, while for a regular black or white hole, $r_e(w) = 2M(w) > a$. Notably, in the static case, the solution falls into the $k = 1$ class, with all dynamic cases belonging to $k = 0$.

TWH analysis parallels RBH's. Irrespective of quantum gravitational effects during its formation, it is presumed that from some stage it is describable by semiclassical gravity. Finite formation time from a distant observer's perspective and absence of curvature singularities are now part of the basic traversability requirements [56]. Ref. [66] demonstrates that dynamical wormholes do not lead to standard Ellis–Morris–Thorne [56] or Simpson–Visser [60] static solutions, while allowed static limits are non-traversable and/or violate the bounds on the NEC violation [24].

Modification of the construction of Ref. [62] allows to bypass this no-go result but faces another obstacle. If the process starts with the metric (23) describing a PBH with $r_+(v) = 2M(v) > a$, then when the decreasing Schwarzschild radius reaches down to a the object becomes a one-way wormhole [60]. Then, if the mass function $M(v) < a/2$ continues to decrease, the solution describes a TWH with the throat at $b_0 = a$. However, if the loss of mass is driven by the Hawking radiation, and its temperature is proportional to κ_K , the Hayward–Kodama surface gravity [67] (see Supplementary Material for details), then as $r_+ = 2M(v) \rightarrow a$ the temperature approaches zero, as $\kappa_K \rightarrow 0$ [17].

Discussion.— Proving the adequacy of a particular ABH model includes disproving its alternatives. A useful step in this direction is constraining their properties, and the results of this work provide such constraints. PBHs, whether or not they possess an event horizon, do not cosmologically couple, likely from the radiation-dominated era. Theoretically, models that depict RBHs with de Sitter cores must reconcile with the equation of state $p = \rho$ near both the inner and outer horizons.

Additional models for singularity avoidance have been proposed. We demonstrate that black-to-white hole transition aligns with semiclassical gravity, but a macroscopic stable remnant, be it a black or white hole, does not. However, the rate of change in its mass remains unconstrained by these general considerations. Beyond the absence of a known mechanism for producing wormholes, their semiclassical existence is restricted by requiring each mouth to develop from an evaporating black hole.

PBHs exhibit remarkable properties distinguishing them from conventional black holes. Translating these properties into observational signatures will enable answering the question of their role in the physical Universe.

Acknowledgments.— PKD, SM, and IS are supported by an International Macquarie University Research Excellence Scholarship. The work of DRT is supported by the ARC Discovery project Grant No. DP210101279. FS is funded by the ARC Discovery project Grant No. DP210101279.

* pravin-kumar.dahal@hdr.mq.edu.au

† swayamsiddha.maharana@hdr.mq.edu.au

‡ fil.simovic@mq.edu.au

§ ioannis.soranidis@hdr.mq.edu.au

¶ daniel.terno@mq.edu.au

- [1] LIGO Scientific Collaboration and Virgo Collaboration, *Astrophys. J. Lett.* **913**, L7 (2021).
- [2] LIGO Scientific Collaboration, Virgo Collaboration, and KAGRA Collaboration, *Phys. Rev. X* **13**, 041039 (2023).
- [3] Event Horizon Telescope Collaboration, *Astrophys. J. Lett.* **875**, L4 (2019).
- [4] Event Horizon Telescope Collaboration, *Astrophys. J. Lett.* **930**, L16 (2022).
- [5] V. Cardoso and P. Pani, *Living Rev. Relativ.* **22**, 4 (2019).
- [6] L. Barack, V. Cardoso, S. Nissanke, and T. P. Sotiriou (eds.), *Class. Quantum Gravity* **36**, 143001 (2019).
- [7] S. W. Hawking and G. F. R. Ellis, *The Large Scale Structure of Space-Time* (Cambridge University Press, Cambridge, England, 1973).
- [8] V. P. Frolov and I. D. Novikov, *Black Holes: Basic Concepts and New Developments* (Kluwer, Dordrecht, 1998).
- [9] V. P. Frolov, arXiv:1411.6981 (2014).
- [10] R. B. Mann, S. Murk, and D. R. Terno, *Int. J. Mod. Phys. D* **31**, 2230015 (2022).
- [11] S. Murk, *Int. J. Mod. Phys. D* **32**, 2342012 (2023).
- [12] P. K. Dahal, F. Simovic, I. Soranidis and D. R. Terno, *Phys. Rev. D* **108**, 104014 (2023).
- [13] É. É. Flanagan and R. M. Wald, *Phys. Rev. D* **54**, 6233 (1996).
- [14] C. Kiefer, *Quantum Gravity* (Oxford University Press, 2012).
- [15] B.-L. Hu and E. Verdaguer, *Semiclassical and Stochastic Gravity: Quantum Field Effects on Curved Spacetime* (Cambridge University Press, Cambridge, England, 2020).
- [16] M. Visser, *Phys. Rev. D* **90**, 127502 (2014).
- [17] R. B. Mann, S. Murk, and D. R. Terno, *Phys. Rev. D* **105**, 124032 (2022).
- [18] P. K. Dahal and D. R. Terno, *Phys. Rev. D* **102**, 124032 (2020).
- [19] P. K. Dahal, S. Maharana, F. Simovic, and D. R. Terno arXiv:2311.02981 (2023).
- [20] V. Faraoni, *Cosmological and Black Hole Apparent Horizons*

- (Springer, Heidelberg, 2015).
- [21] V. Faraoni, A. Giusti, and B. H. Fahim, *Phys. Rep.* **925**, 1 (2021).
- [22] V. Faraoni, G. F. R. Ellis, J. T. Firouzjaee, A. Helou, and I. Musco, *Phys. Rev. D* **95**, 024008 (2017).
- [23] S. Dodelson and F. Schmidt, *Modern Cosmology* (Elsevier, 2021).
- [24] E.-A. Kontou and K. Sanders, *Class. Quantum Gravity* **37**, 193001 (2020).
- [25] S. A. Hayward, *Phys. Rev. Lett.* **96**, 031103 (2006).
- [26] P. K. Dahal, S. Murk, and D. R. Terno, *AVS Quantum Sci.* **4**, 015606 (2022).
- [27] S. Murk and I. Soranidis, *Phys. Rev. D* **108**, 124007 (2023).
- [28] Planck collaboration, *Astr. Astrophys.* **641**, A6 (2020).
- [29] S. Akcay and R. A. Matzner, *Quant. Class. Grav.* **28**, 085012 (2011).
- [30] M. Cadoni, R. Murgia, M. Pitzalis, and A. P. Sanna, *arXiv:2309.16444* (2023).
- [31] K. S. Croker, M. Zevin, D. Farrah, K. A. Nishimura1, and G. Tarlé, *Astr. J. Lett.* **921**, L22 (2021).
- [32] D. Farrah, K. S. Croker, M. Zevin, G. Tarlé *et al.*, *Astr. J. Lett.* **944**, L31 (2023).
- [33] C. L. Rodriguez, *Astr. J. Lett.* **947**, L12 (2023).
- [34] L. Lei *et al.*, *arXiv:2305.03408* (2023).
- [35] R. Andrae and K. El-Badry, *Astron. Astrophys.* **673**, L10 (2023).
- [36] M. Cadoni, A.P. Sanna, M. Pitzalis, B. Banerjee, R. Murgia, N. Hazrac, and M. Branchesic, *J. Cosmol. Astropart. Phys.* **11**, 007 (2023).
- [37] P. P. Avelino, *J. Cosmol. Astropart. Phys.* **08**, 005 (2023).
- [38] S. L. Parnovsky, *arXiv:2302.13333* (2023).
- [39] R. Gaur and M. Visser, *arXiv:2308.07374* (2023).
- [40] E. Curiel, *Nat. Astron.* **3**, 27 (2019).
- [41] M. Yu. Khlopov, *Res. Astron. Astrophys.* **10**, 495 (2010).
- [42] C.-M. Yoo, *Galaxies* **10**, 112 (2022).
- [43] V. P. Frolov and G. A. Vilkovisky, *Phys. Lett. B* **106**, 307 (1981).
- [44] A. Ashtekar and M. Bojowald, *Class. Quantum Gravity* **22**, 3349 (2005).
- [45] M. Bojowald, R. Goswami, R. Maartens, and P. Singh, *Phys. Rev. Lett.* **95**, 091302 (2005).
- [46] D. Malafarina, *Universe* **3**, 48 (2017).
- [47] A. Ashtekar, *Universe* **6**, 21 (2020).
- [48] H. M. Haggard and C. Rovelli, *Phys. Rev. D* **92**, 104020 (2015).
- [49] C. Rovelli, *Nature Astr.* **1**, 0065 (2017).
- [50] E. Bianchi, M. Christodoulou, F. D’Ambrosio, H. M. Haggard, C. Rovelli, *Class. Quantum Grav.* **35**, 225003 (2018).
- [51] C. Rovelli and F. Vidotto, *Universe* **4**, 127 (2018).
- [52] P. Martin-Dussaud and C. Rovelli *Class. Quantum Grav.* **36**, 245002 (2019).
- [53] J. Ben Achour, S. Brahma, S. Mukohyamaa, and J-P. Uzand, *J. Cosmol. Astropart. Phys.* **09**, 020 (2020).
- [54] R. Carballo-Rubio, F. Di Filippo, S. Liberati, C. Pacilio, and M. Visser, *J. High Energy Phys.* **09**, 118 (2022).
- [55] M. Han, C. Rovelli, and F. Soltani, *Phys. Rev. D* **107**, 064011 (2023).
- [56] M. Visser, *Lorentzian Wormholes: From Einstein to Hawking* (American Institute of Physics, Woodbury, USA, 1996).
- [57] S. Krasnikov, *Back-in-Time and Faster-than-Light Travel in General Relativity* (Springer, New York, 2018).
- [58] T. Damour and S. N. Solodukhin, *Phys. Rev. D* **76**, 024016 (2007).
- [59] V. Cardoso, E. Franzin, and P. Pani, *Phys. Rev. Lett* **116**, 171101 (2016).
- [60] A. Simpson and M. Visser, *J. Cosmol. Astropart. Phys.* **02**, 042 (2019).
- [61] K. A. Bronnikov, *Phys. Rev. D* **106**, 064029 (2022).
- [62] A. Simpson, P. Martín-Moruno, and M. Visser, *Class. Quantum Grav.* **36**, 145007 (2019).
- [63] D. Hochberg and M. Visser, *Phys. Rev. Lett.* **81**, 746 (1998).
- [64] S. A. Hayward, *Phys. Rev. D* **79**, 124001 (2009).
- [65] D. D. McNutt, W. Julius, M. Gorban, B. Mattingly, P. Brown, and G. Cleaver, *Phys. Rev. D* **103**, 124024 (2021).
- [66] D. R. Terno, *Phys. Rev. D* **106**, 044035 (2022).
- [67] S. A. Hayward, *Class. Quantum Gravity* **15**, 3147 (1998).
- [68] S. A. Hayward, *Phys. Rev. D* **49**, 6467 (1994).

SUPPLEMENTARY MATERIAL

Self-consistent approach and physical black holes

To ensure the absence of scalar curvature singularities we use two quantities that can be expressed directly from EMT components,

$$\tilde{\mathbb{T}} := T^\mu_\mu, \quad \tilde{\mathfrak{T}} := T^\mu_\nu T^\nu_\mu. \quad (24)$$

The Einstein equations relate them to the curvature scalars as $\tilde{\mathbb{T}} \equiv -R/8\pi$ and $\tilde{\mathfrak{T}} \equiv R^\mu_\nu R^\nu_\mu/64\pi^2$. It is possible to show that the component T^θ_θ can introduce only sub-leading divergencies, and only the finite values of

$$\mathbb{T} = (\tau^r - \tau_t)/f, \quad \mathfrak{T} = ((\tau^r)^2 + (\tau_t)^2 - 2(\tau_t^r)^2)/f^2, \quad (25)$$

need to be ensured. From Eqs. (8)–(10) it follows that the cosmological constant drops out of the consideration of the potentially divergent parts of the effective EMT components.

For $k = 0$ solutions the (tr) block of the EMT near the Schwarzschild radius of (an evaporating) PBH is

$$T^a_b = \begin{pmatrix} \Upsilon^2/f & e^{-h}\Upsilon^2/f^2 \\ -e^h\Upsilon^2 & -\Upsilon^2/f \end{pmatrix}, \quad T_{\hat{a}\hat{b}} = -\frac{\Upsilon^2}{f} \begin{pmatrix} 1 & 1 \\ 1 & 1 \end{pmatrix}, \quad (26)$$

where the second expression is written in an orthonormal frame [10].

Using the (v, r) coordinate the metric functions near the (outer) apparent horizon of a PBH can be written as

$$C_+(v, r) = r_+(v) + w_1(v)y + \mathcal{O}(y^2), \quad (27)$$

$$h_+(v, r) = \chi_1(v)y + \mathcal{O}(y^2), \quad (28)$$

where $y := r - r_+$. By its definition $w_1 \leq 1$. It is exactly zero for Vaidya-like metrics and $w_1 = 1$ for $k = 1$ dynamical solutions that describe the first moment of formation (and, possibly, the last moment of existence) of the trapped region [10, 12].

The Hayward–Kodama surface gravity is defined by using the Kodama vector field \mathbb{k} imitating the properties of the

Killing vector-based surface gravity [67],

$$\frac{1}{2} \mathbb{k}^\mu (\nabla_\mu \mathbb{k}_\nu - \nabla_\nu \mathbb{k}_\mu) =: \kappa_{\mathbb{K}} \mathbb{k}_\nu, \quad (29)$$

evaluated on the apparent horizon. Hence it is explicitly given by

$$\kappa_{\mathbb{K}} = \frac{1}{2} \left(\frac{C_+(v, r)}{r^2} - \frac{\partial_r C_+(v, r)}{r} \right) \Big|_{r=r_+} = \frac{(1 - w_1)}{2r_+}. \quad (30)$$

Useful cosmological coordinate transformations

A careful use of relations between different useful coordinate systems is required to study properties of cosmological black holes [12, 20, 39]. Here we demonstrate how a metric of Eq. (2) with the MSH mass $C_M = C + H^2 r^3$ (and the metric function given by Eqs. (16)) can be transformed into a form that makes it obvious that a PBH is embedded in an exponentially expanding flat FLRW universe,

$$ds^2 = -d\tau^2 + a^2(\tau) (d\chi^2 + \chi^2 d\Omega_2). \quad (31)$$

As the first step we perform a transformation to the Painlevé–Gullstrand coordinates [8, 20, 39] via

$$dt = e^{-h} (\mathfrak{A} d\tau + \mathfrak{B} dr), \quad (32)$$

where $\mathfrak{B} = \sqrt{C_M(\tau, r)/r}/f$ is chosen to eliminate the pre-factors of dr^2 , and \mathfrak{A} is the integrating factor,

$$\partial_r (e^{-h} \mathfrak{A}) = \partial_\tau (e^{-h} \mathfrak{B}). \quad (33)$$

For transformations of any metric with C and h independent from t (and in particular pure de Sitter or Schwarzschild–Kottler–de Sitter spacetimes), we set $dt = d\tau + e^{-h} \mathfrak{B} dr$. We expect $\mathfrak{A} \approx 1$ for $r_g \ll r$. The Painlevé–Gullstrand form of the metric is

$$ds^2 = -\mathfrak{A}^2 d\tau^2 + \left(dr - \mathfrak{A} \sqrt{C_M/r} d\tau \right)^2 + r^2 d\Omega_2. \quad (34)$$

A the second step the areal radius is expressed as $r = a\chi = a_0 e^{H\tau} \chi$ and the metric becomes

$$ds^2 = -\mathfrak{A}^2 d\tau^2 + a^2 \chi^2 d\Omega_2 + a^2 \left(d\chi + \left[H\chi - \mathfrak{A} \sqrt{\frac{C_M}{a^3 \chi}} \right] d\tau \right)^2. \quad (35)$$

Taking into account that for $r = a\chi \gg r_g$,

$$\sqrt{\frac{C_M}{\chi a^3}} = H\chi - \frac{1}{2Ha} \frac{C}{r^2} + \mathcal{O}(r^{-5}), \quad (36)$$

and the metric approaches Eq. (31)

Physical white holes

The spherically symmetric metric with $r'_g > 0$ describes a regular growing white hole, with timelike anti-trapping horizons bounding the anti-trapped region. In (u, r) coordinates, the line element in the near-horizon region is well-described by

$$ds^2 = -f(u, r) du^2 - 2du dr + r^2 d\Omega_2^2. \quad (37)$$

A singularity is avoided by introducing an inner horizon, arising from the introduction of a minimal length scale. A useful model is obtained starting with such a static regular white hole, we promote it to a dynamical one where the evolution will be described by the retarded coordinate u . We consider the following metric function

$$f(u, r) = g(u, r) (r - r_-(u))^3 (r - r_+(u)), \quad (38)$$

where $r_+(u)$ is the outer anti-trapping horizon, $r_-(u)$ is the inner anti-trapping horizon, and $g(u, r)$ is a positive function given by

$$g(u, r)^{-1} = r^4 - 3r_- r^3 + (4r_-^2 + 3r_- r_+) r^2 + (-3r_-^2 r_+ - r_-^3) r + r_-^3 r_+. \quad (39)$$

This metric was proposed in Ref. [54] as a means to cure the mass inflation instability problem at the expense of a degenerate inner horizon with vanishing surface gravity. We prescribe an evolution of the inner and outer apparent horizons consistent with the assumptions given above. This implies both horizons must grow, and the two solutions to $r_+(u) = r_-(u)$ describe the formation and disappearance points which occur in an extremal limit [27].

Black-to-white hole transition

Majority of the RBH models exhibit the property of $h_+(v, r) = 0$, and we limit our consideration to this particular case. Two key assumptions allow us to make generic statements about the form of the metric function defining a RBH. Firstly, the trapped region, bounded by the outer apparent horizon $r_+(v)$, must be present. Following the definitions of Ref. [20, 68] the existence of such a region is equivalent to having $\theta_- \theta_+ > 0$, where θ_- and θ_+ represent the expansions of ingoing and outgoing rays, respectively. Secondly, ensuring the regularity of the spacetime necessitates the introduction of a minimal length scale, which possibly originates from quantum gravity effects restricted within a finite region. This leads to the presence of an inner horizon $r_-(v)$ serving as an additional boundary of the trapped region, satisfying $r_- < r_+$.

Taking into consideration the above properties, we restrict the metric function of the RBH to the form:

$$f(v, r) = g(v, r)(r - r_-(v))^a(r - r_+(v))^b, \quad (40)$$

where $g(v, r) > 0$ is an appropriate function, providing a regular center as well as the desired asymptotic behavior, and a, b are positive odd integer numbers, describing the degree of each horizon's degeneracy [27]. According to our analysis, both horizons must decrease in radius and the sole way for the trapped region to vanish is by their merging at a specific time v_* , i.e. $r_+(v_*) = r_-(v_*)$. At this moment, which is depicted as a gray disk in Fig. 2, we have that

$$\theta_- \theta_+|_{v_*} = -\frac{2}{r^2} g(v_*, r)(r - r_*(v_*))^{a+b} \leq 0, \quad (41)$$

signifying the disappearance of the trapped region.

Simultaneously, at this instant of time ($u_* = v_*$), the transition to a white hole occurs. Following this transition, the dynamical evolution, reminiscent of the RBH case, is described in retarded coordinates to align with the definition of a white hole, as indicated by their expansions. Therefore, the metric function takes the form:

$$\tilde{f}(u, r) = \tilde{g}(u, r)(r - \tilde{r}_-(u))^{\tilde{a}}(r - \tilde{r}_+(u))^{\tilde{b}}. \quad (42)$$

The primary distinction to the RBH case lies in the expand-

ing nature of the anti-trapping horizons. The termination of this expansion is possible in a similar manner to the termination of the RBH evaporation. There exists a moment in time, u_f , where these anti-trapping horizons merge, i.e. $\tilde{r}_+(u_f) = \tilde{r}_-(u_f)$. Justifying the disappearance of the anti-trapped region is once again based on the sign of the expansions' product: $\theta_- \theta_+|_{u_f} \leq 0$.

Some properties of the Simpson–Visser metric

For the MSH mass $C_M(v, r) = 2M(v) + a^2(r - 2m(v))/r^2$ the equation $f(v, r) = r$ has two positive roots $r_1 = 2M$ and $r_2 = a$. For $M > a/2$ (black hole), the expansion of Eq. (27) gives

$$C = 2M + \frac{a^2}{4M^2}y + \mathcal{O}(y^2), \quad (43)$$

i.e., $r_+ = 2M(v)$ and $w_1 = a^2/r_+$. For $M < a/2$ (worm-hole),

$$C = a + (4M - a)y/a + c\mathcal{O}(y^2), \quad (44)$$

i.e., $r_+ = a$ and $w_1 = 4M/a - 1$. Eq. (30) implies that at the transition $a = 2M$ the surface gravity $\kappa_K = 0$.